Journal of Luminescence 241 (2022) 118486

Contents lists available at ScienceDirect

Journal of Luminescence

journal homepage: www.elsevier.com/locate/jlumin

Structural, optical and luminescence properties of $BaLaGa_3O_7$: x Eu^{3+} ceramic phosphors

B. Vasanthi [a,b], N. Gopakumar [b], P.S. Anjana [a,*]

[a] PG Department of Physics, All Saints' College, University of Kerala, Thiruvananthapuram, Kerala, 695007, India
[b] PG Department of Physics and Research Centre, Mahatma Gandhi College, University of Kerala, Thiruvananthapuram, Thiruvananthapuram, Kerala, 695004, India

ARTICLE INFO

Keywords:
Barium lanthanum gallate
Photoluminescence
Mechanoluminescence
Thermoluminescence

ABSTRACT

The undoped and Eu^{3+} doped $BaLaGa_3O_7$ ceramic phosphors have been prepared using solid state reaction technique. The structural studies have been done using X-ray Diffraction (XRD) and Fourier transform infra-red (FTIR) technique and the surface morphology analysis using Field emission scanning electron microscope (FESEM). The elemental analysis has been carried out using Energy Dispersive X-ray spectroscopy (EDX) and elemental mapping. XRD study reveals that all the prepared phosphors are single phase with tetragonal crystal structure. The FESEM and EDX spectra confirm the single phase nature of the phosphors. FTIR technique identifies the various vibrational modes present in the prepared phosphors. The UV–Visible analysis provides the absorption region and band gap energies of undoped as well as doped $BaLaGa_3O_7$ phosphors. The photoluminescence (PL) excitation spectra consist of sharp excitation peaks of Eu^{3+} ions at 374 and 394 nm. The emission spectra corresponding to excitation wavelengths of 374 and 394 nm have been carried out. Maximum PL emission is obtained for excitation at 374 nm and it provides excellent orange red emission. The decay profile of $BaLaGa_3O_7$:xEu^{3+} phosphors have been carried out. The mechanoluminescence (ML) property of the doped phosphors reveals good ML emission without any pre irradiation. The information about the trap depth parameters and charge carriers in the 1 kGy irradiated $BaLaGa_3O_7$ phosphor has been studied using the thermoluminescence (TL) glow curves. The $BaLaGa_3O_7$ phosphor is having kinetics of first order with activation energy 1.107 eV.

1. Introduction

The compound of general formula ABC_3O_7 where A = Ca, Sr, Ba, B = Y, La, Gd, C = Al, Ga are widely used in light emitting applications as well as lasing possibilities [1,2]. They exist in two structural forms, orthorhombic (C_{2V}) and tetragonal (C_{4V}) [3,4]. In ABC_3O_7, A and B atoms are eight fold coordinated and they occupy the same lattice site whereas C atom is tetrahedrally coordinated and enter the crystal lattice into two different positions. The crystal has C_3O_7 sheets in a - b plane partitioned by A and B atoms [3,5]. Lanthanum gallate has unique combination of thermal, electrochemical and optical properties which makes it promising for optoelectronic applications. This type of crystals doped with the trivalent rare earth ions are used to predict the orientation and symmetry of the materials like $BaLaGa_3O_7$, $SrLaGa_3O_7$, and $SrGdGa_3O_7$ [6]. Preparation of polycrystalline $BaLaGa_3O_7$ has been first reported by Ismatov and co-workers [7] and further work on this crystal has been done by Piekarczyk et al. using Czocharalski method for evaluating its refractive indices, elastic, piezoelectric and dielectric properties [7,8].

They found that material belong to space group P-42$_1$m with tetragonal melilite crystal structure [8,9]. $BaLaGa_3O_7$ doped with neodymium has been reported by W. Ryba- Romanowski et al. and focused on the properties of high laser threshold as well as low laser efficiency of this material [10]. The gallium oxide is one of the widest band gap materials. Ga_2O_3 with suitable rare earth oxide mainly in the form of RE_2O_3 are very useful in the field of luminescent devices, optical transmission, biochemical probes, field emission displays etc due its excellent chemical, electronic and optical properties which is provided by the presence of 4f electrons [11,12]. Rare earth (RE^{3+}) doped phosphors exhibits intense emission of light, long life time, high quantum yield and better optical properties because of their chemical and thermal stability, high luminescence and color purity [13]. There are different kinds of rare earth materials, in which phosphors doped with Eu^{3+} acts as a promising candidate for the illumination technology. This is due to

* Corresponding author.
E-mail address: psanjanaa@yahoo.com (P.S. Anjana).

https://doi.org/10.1016/j.jlumin.2021.118486
Received 18 December 2020; Received in revised form 8 September 2021; Accepted 16 September 2021
Available online 1 October 2021

the intra 4f - 4f transition between excited states to ground state. The emission spectra of europium ion is ascribed due to transitions from excited $^5D_0 \rightarrow {}^7F_j$ (j = 0, 1, 2, 3, 4) levels of Eu^{3+} ions. The intense bright red emission is provided by the forced electric dipole transition from $^5D_0 \rightarrow {}^7F_2$ of Eu^{3+} [13–15].

Mechanoluminescence (ML) is a kind of luminescence exhibited by some solid materials due to the impact of mechanical action induced in it. ML can be excited by compressing, stretching, bending, loading, shaking, cutting, cleaving, grinding, scratching, crushing or impulsive deformation of solids [16–18]. Mechanoluminescence has emerged as an important topic for the research due to its wide range of applications in impact sensors, fracture sensor, damage sensor, sensor for stress indicators, self-diagnosis systems, wireless fracture sensor systems, ML paints in crack detecting devices etc [18–20]. A lot of works has been reported on the mechanoluminescence of Eu^{3+} doped aluminate based compounds. Sajan et al. has been reported the mechanoluminescence properties of europium doped zinc barium aluminate and (1-x) Mgo. xBao-Al_2O_3 phosphors [19,20]. B.P Chandra et al. has reported the immense ML emission of rare earth ions doped strontium aluminate phosphors [21]. The mechanoluminescence in silicates have been reported by Ishwar Prasad Sahu et al. in europium ion doped strontium metasilicates [22] and Ravi Shrivastava et al. has investigated in $Sr_2MgSi_2O_7$:Eu^{2+}, Dy^{3+} phosphors [23]. The mechanoluminescence properties of Eu^{3+} ions doped in $CaZrO_3$ phosphors has been reported by Ishwar Prasad Sahu et al. [24] and in $Ca_2Gd_2W_3O_{14}$ phosphors has been investigated by S. Sailaja et al. [25]. But mechanoluminescence of barium lanthanum gallate phosphor doped with Eu^{3+} ions are not yet reported.

Metallic oxide based thermoluminescent materials attracts the scientific as well as medical field due to its enormous applications in medical physics which includes radiotherapy, radio diagnostic, nuclear medicine, radiation protection [26]. It also finds its applications in industry, age determination, geology or solid state defect structure analysis, dosimetry and archeological dating [27,28]. Thermoluminescence is a type of luminescence in which thermally stimulated light is emitted by the absorption of energy from ionizing radiations. The radiations cause displacement of electrons within the crystal lattice of the substance. Upon heating, the trapped electrons return to their normal lower-energy positions, releasing energy [18,22]. The thermoluminesence analysis is very informative for understanding the life time of an electron which can stay in the trap created in the phosphors [28]. S.J Dhoble and co-workers investigated the thermoluminescence properties of Eu^{3+} doped $SrYAl_3O_7$ having the general chemical composition ABC_3O_7 using combustion method and reported the excellent TL emission of this phosphor [29].

Lanthanum gallate and alkaline earth based lanthanum gallate ceramic phosphors and its applications [30] had been copiously discussed in literature. A few attempts have been made to study the properties of $BaLaGa_3O_7$ prepared using Czocharalski method. The barium lanthanum gallate phosphor is a promising host lattice for trivalent lanthanide ion dopants for the preparation of lasing as well as luminescent materials. Hence the present investigation reports the preparation of europium doped barium lanthanum gallate phosphor using solid state reaction technique and studies its photoluminescence (PL), mechanoluminescence (ML) and thermoluminescence (TL) properties.

2. Experimental techniques

2.1. Sample preparation

$BaLaGa_3O_7$: xEu^{3+} (x = 0, 0.02, 0.05, 0.08 and 0.1 mol %) phosphors were prepared using conventional solid state method. The stoichiometric amounts of $BaCO_3$ (99.6%, Sigma Aldrich), La_2O_3 (99.9%, Alfa Aesar), Ga_2O_3 (99.99%, Alfa Aesar), Eu_2O_3 (99.99%, Alfa Aesar), were taken as raw materials and mixed for 2 h in an agate mortar and pestle with distilled water as medium. It is dried in an oven and then transferred into a platinum crucible and calcined at optimum temperature of 1200 °C for 5 h at a heating rate of 10 °C/min. The calcined powder is then ground for characterization.

2.2. Powder characterization

The phase analysis of the phosphors was done with X-ray diffraction technique on powder samples using a Bruker AXS D8 Advanced X-ray diffractometer. The pattern was collected over 2Θ ranging 10–80° with a step size of 0.01° and a scanning rate 4.0°/min using CuKα radiation (λ = 1.54 Å). Fourier transform infrared spectra were recorded using PerkinElmer FTIR/FIR Spectrometer in the range 400–4000 cm^{-1}. The microstructure and surface morphology of the prepared phosphors were analyzed using Nova NanoSEM 450 UoK Field Emission Scanning Electron Microscope (FEI, USA). The prepared phosphors were coated with thin layer of gold and then surface morphology of the phosphors were investigated. The energy dispersive X-ray spectroscopic (EDX) and its elemental mapping were carried out for the elemental analysis and its distribution using Carl Zeiss EVO 18 Research. Absorption spectra were recorded in the range of 200–800 nm and their band gap energy was determined using PerkinElmer UV/VIS/NIR Spectrometer Lamda 950. Photoluminescence excitation and emission characteristics were examined by a Fluorescence Spectrophotometer (Fluorolog Horiba) equipped with a monochromator and a Xenon lamp. The decay profiles of the phosphors were recoded using EDINBURGH FLS 1000 under the excitation of 374 and emission wavelength of 616 nm. The ML emission from the doped phosphors without any pre-irradiation of UV or gamma rays were monitored by an indigenous set-up having photomultiplier tube (PMT 931A) positioned below the Lucite plate and connected to a digital storage oscilloscope. ML was excited by the hitting of a load of mass 100 g on to the doped phosphor from different heights using a guiding cylinder. The impact velocity was calculated using the equation $(2gh)^{1/2}$. The TL spectrum is recorded using Nucleonix make TLD reader with heating performed up to 400 °C and heating rate under thermal stimulation is varied up to 5 °C/s.

3. Results and discussion

3.1. X-ray diffraction (XRD)

Powder XRD patterns of $BaLaGa_3O_7$: xEu^{3+} (x = 0, 0.02, 0.05, 0.08, 0.1 mol %) phosphors are shown in Fig. 1. All the diffraction peaks of the synthesized phosphors are in good agreement with standard ICDD card no.01-083-0963. No other secondary phase is observed. It indicates that as synthesized phosphor has a single phase with tetragonal structure and space group of this phosphor is P-421m (113) [31]. No other characteristic peaks of Eu^{3+} ions are identified due to small doping concentration and hence there is no significant change in the crystal structure of host lattice after the incorporation of europium ions [31]. There is no significant shift in the position of diffraction peaks for Eu^{3+} doped phosphors. The typical diffraction peaks are obtained at 27.42°, 29.59°, 33.20°, 34.78°, 48.83°, 57.77° and 63.74° identified as (201), (211), (002), (310), (312), (213) and (521) planes of the host lattice respectively.

3.2. Microstructural analysis

Fig. 2(a)–(c) show the microstructure and morphological properties of undoped, 0.05 and 0.1 mol % of Eu^{3+} doped barium lanthanum gallate phosphors. From the FE-SEM images, the synthesized compounds are made up of two different sized particles - small particles with size around 1–3 μm and large particles with an average size of about 2–5 μm respectively. Doping of Eu^{3+} ions into the host lattice does not induce a significant change in crystal morphology but the different sized particles can be seen very clearly with increase in Eu^{3+} ions concentrations [13,

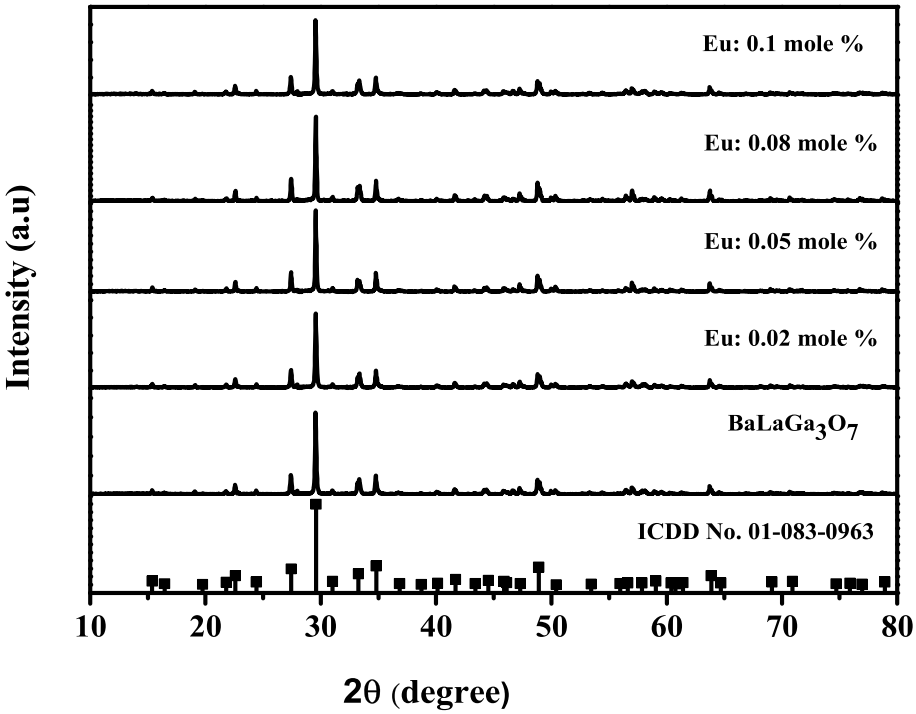

Fig. 1. XRD Patterns of undoped and Eu^{3+} ions doped $BaLaGa_3O_7$ phosphors.

22].

The chemical composition and homogeneity of the undoped and 0.05 mol % of Eu^{3+} doped barium lanthanum gallate phosphors has been characterized using energy dispersive X-ray (EDX) analysis and elemental mapping technique for overall area and spot mode analysis. The EDX spectra corresponding to the spot mode analysis at smaller grain as well as larger grain present in the undoped $BaLaGa_3O_7$ phosphor are shown in Fig. 3(a–b). The EDX spectra at these two different sized particles reveal the existence of same chemical composition and the presence of Ba, La, Ga and O in the synthesized phosphor's surface [13]. Fig. 3(c–d) represent the EDX spectra of 0.05 mol % of Eu^{3+} doped $BaLaGa_3O_7$ phosphor. Here also the constituent elements Ba, La, Ga, O, Eu with almost same composition are confirmed in smaller and larger grain using spot mode analysis [28]. The EDX spectral analysis of undoped and 0.05 mol % of Eu^{3+} doped $BaLaGa_3O_7$ phosphors are given in Table 1.

EDX elemental mapping corresponding to the overall area for undoped $BaLaGa_3O_7$ phosphor is shown in Fig. 4(a–f) and 0.05 mol % of Eu^{3+} doped mapping are shown in Fig. 5(a–g). Elemental mapping exhibit the presence and homogeneous distribution of all the constituent elements such as Ba, La, Ga, and O in $BaLaGa_3O_7$ phosphor and similar distributions of the constituent elements Ba, La, Ga, O and Eu are observed in $BaLaGa_3O_7$: $0.05Eu^{3+}$ phosphor [13]. The elemental mapping provides information about the presence of all constituent elements associated with the preparation of these phosphors and the successful incorporation of europium ions into the $BaLaGa_3O_7$ lattice. This result is good agreement with the XRD result.

3.3. Fourier transform infrared spectra (FTIR)

The Fourier Transform Infra-Red spectroscopy provides the characteristics of the elements and vibrational bands present in the phosphors [32]. The FTIR spectra of undoped and Eu^{3+} doped phosphors are shown in Fig. 6. It is clear that the spectrum of $BaLaGa_3O_7$ is slightly different from the doped one. The small shift in the band position is attributed due to the incorporation of the europium ion. The bands slightly shifted to the higher wavelength region with the concentration of Eu^{3+} ions. The band appeared at 567 cm^{-1} in undoped $BaLaGa_3O_7$ phosphor absent in doped phosphors [see inset of Fig. 6]. The factors affecting the absorption bands are homogeneity of the chemical bonding, presence of dopants and bond strain. In the case of doped phosphors, the presence of Eu^{3+} ion may cause some defects in the host lattice [32]. This defect can affect the strength of the chemical bonds and small shift in positions may occur. In some cases broadening of absorption bands take place. The band at 567 cm^{-1} disappears due to the presence of Eu^{3+} ions and that band get broaden to a single absorption band in doped phosphors [32]. The band at ~420 cm^{-1} is assigned to Ga–O bending vibration. The region ~485 cm^{-1} assigned the O–Ga - O bending mode [33–35]. Assignments of the absorption bands show that the bands for Ba–O are located in the range of ~525 cm^{-1} [36]. The region 567 cm^{-1} is the Ba–O stretching mode [37–39]. The wave number in the range ~670 cm^{-1} is the presence of Ga–O stretching vibrational mode in the barium lanthanum gallate lattice [34,35]. Also stretching vibration bands of La–O is observed in the range ~650 cm^{-1} [40]. The band at ~740 cm^{-1} is assigned to the stretching and bending of GaO_4 units [33–35]. The band at ~870 cm^{-1} is due to the La–O bonds as well as the presence of Ba–O bonds presents in the system [41,42]. If any functional groups like O–H, C–H, N–H present in the phosphor, it can decrease the intensity of the luminescence emission of the phosphors. The presence of such functional groups can form new defects on the phosphors surface which can act as a source of quencher on luminescence intensity. But in the present study, the starting reagents are completely oxides and carbonates. Due to high temperature synthesis, the oxides and carbonates are removed and also there are no other functional groups that exist in the phosphors. The O–H bond is very weak in both undoped and doped phosphors and it can be clearly seen in FTIR spectra. These phosphors can exhibit good luminescence properties due to the presence of less impurity [34]. The band assignments are tabulated in Table 2.

3.4. UV–visible studies

The optical absorption measurement is one of the important factors for the determination of band structure as well as the band gap energy of the prepared $BaLaGa_3O_7$: xEu^{3+} ceramic phosphors. Fig. 7 represents the

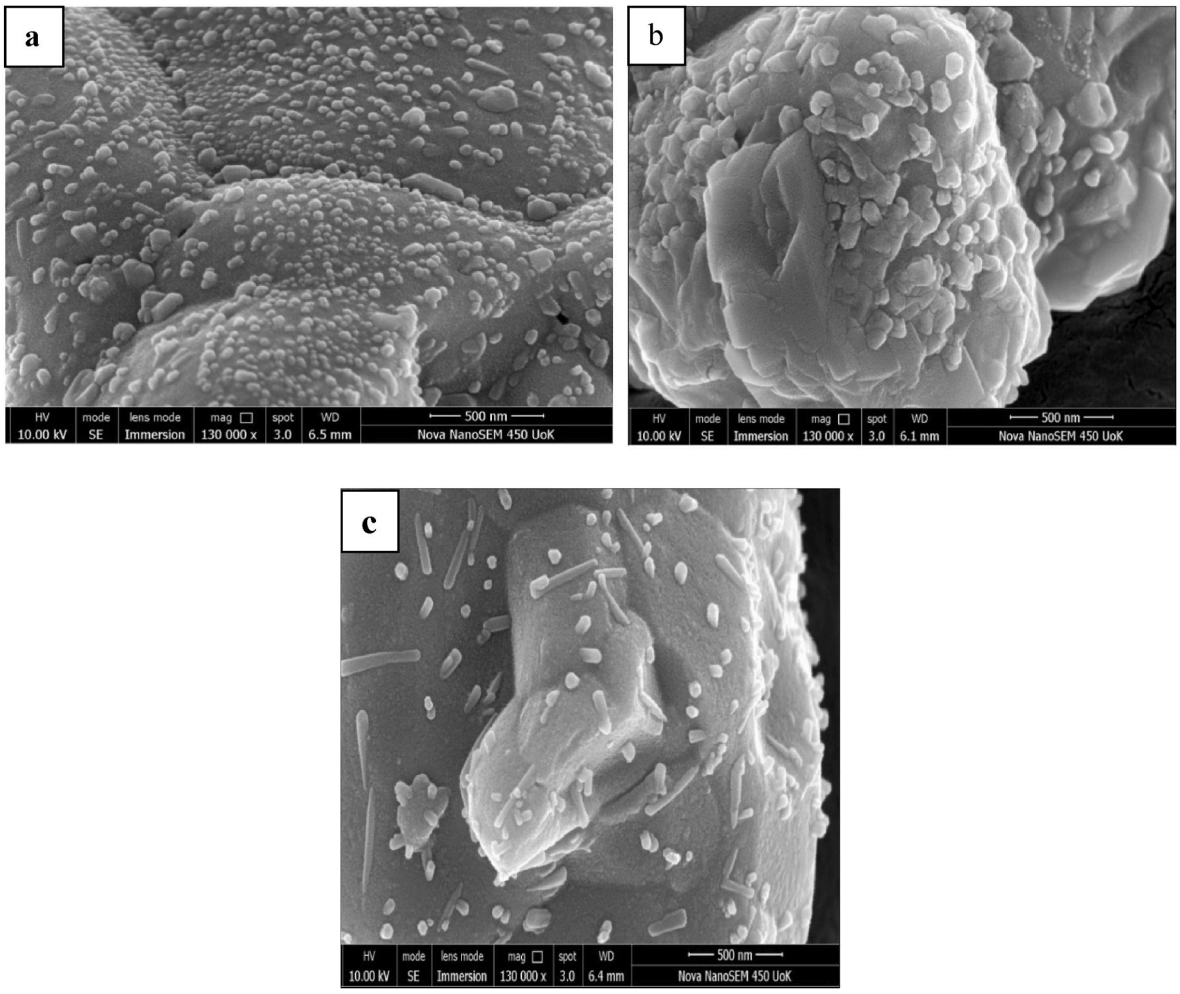

Fig. 2. FESEM image of a) undoped $BaLaGa_3O_7$ phosphor b) 0.05 mol % c) 0.1 mol % of Eu^{3+} ions doped $BaLaGa_3O_7$ phosphors.

UV–Visible absorption spectra of undoped as well as doped barium lanthanum gallate phosphors. The absorption spectra reveal that the maximum absorption occurs in the range 300–350 nm and absorption peaks are recorded at 375 ($^7F_0 \rightarrow {}^5L_7$), 386 ($^7F_0 \rightarrow {}^5G_4$) and 394 nm ($^7F_0 \rightarrow {}^5L_6$) assigned to the Eu^{3+} ions transition (inset of Fig. 7) [43]. The variation recorded in the direct band gap values with different Eu^{3+} concentrations are shown in Fig. 7a. The band gap energy of phosphor describes the energy required to excite an electron. The energy - dependent absorption coefficient α can be expressed by the Tauc method using the equation.

$$(\alpha\, h\nu)^{1/n} = c\left(h\nu - E_g\right) \quad (1)$$

where hν is the photon energy and α is the absorption edge, the value of α is obtained from absorption spectra, E_g is the band gap energy and c is a constant. The value of n depends on the nature of the electron transition and is equal to 1/2 or 2 for the direct and indirect allowed transition respectively [37,44]. The direct band gap energy of $BaLaGa_3O_7$ phosphor is calculated to be 4.29 eV (inset of Fig. 7a). In $BaLaGa_3O_7$ phosphor, gallium oxide acts as the luminescent centre [13]. Junling Meng et al. (2016) have been reported the insulator nature and wide band gap of $BaLaGa_3O_7$ phosphor. In single crystalline $BaLaGa_3O_7$ phosphor, the valence band is ascribed due to 2p orbital of Ga–O bond and the conduction band is emerged from the 5d orbitals of Barium (Ba) and Lanthanum (La) ions [2]. The direct band gap energies of Eu^{3+} doped phosphors are calculated to be 4.53, 4.60, 4.58 and 4.55 eV respectively for 0.02, 0.05, 0.08 and 0.1 mol % of Eu^{3+} doped $BaLaGa_3O_7$ phosphors. It is observed that with increasing Eu^{3+} concentrations, an increase in the optical band gap energies up to 0.05 mol % of Eu^{3+} ion concentration and then value decreases. The increase in the band gap values with Eu^{3+} doping on $BaLaGa_3O_7$ can be explained on the basis of Burstein – Moss effect. The Fermi level of barium lanthanum gallate lies between conduction and valence band. The presence of europium ion increases the concentration of electron carriers within the conduction band and hence a positive shift occurs in the fermi level present in the conduction band. This may cause more energy to excite the electron from the valence band to conduction band. This results in the increment of band gap energy due to filling of states near the bottom of the conduction band [45–48].

3.5. Photoluminescence studies

Fig. 8 represents the emission spectrum of undoped barium lanthanum gallate phosphor. The excitation spectrum of the prepared ceramic exhibits strong excitation peak at 275 nm (inset of Fig. 8). The emission spectrum of $BaLaGa_3O_7$ phosphor shows a strongest emission band centered at 413 nm and less intense peak in the 495 nm corresponds to the blue region of the visible spectrum. In barium lanthanum gallate phosphor, Ga^{3+} ions present in the tetrahedral site acts as a self - activated luminescent center. Lammers et al. (1986) and Junling Meng et al. (2016) reported that the blue emission in pure barium lanthanum gallate happens when an electron from an O^{2-} vacancy or from the Ga^{3+} center recombines with trapped holes. Ga^{3+} ions in the host lattice can capture electrons that are knocked out from the O^{2-} ion. Ga^{3+} ions combine with UV-generated free electrons that are produced in oxygen

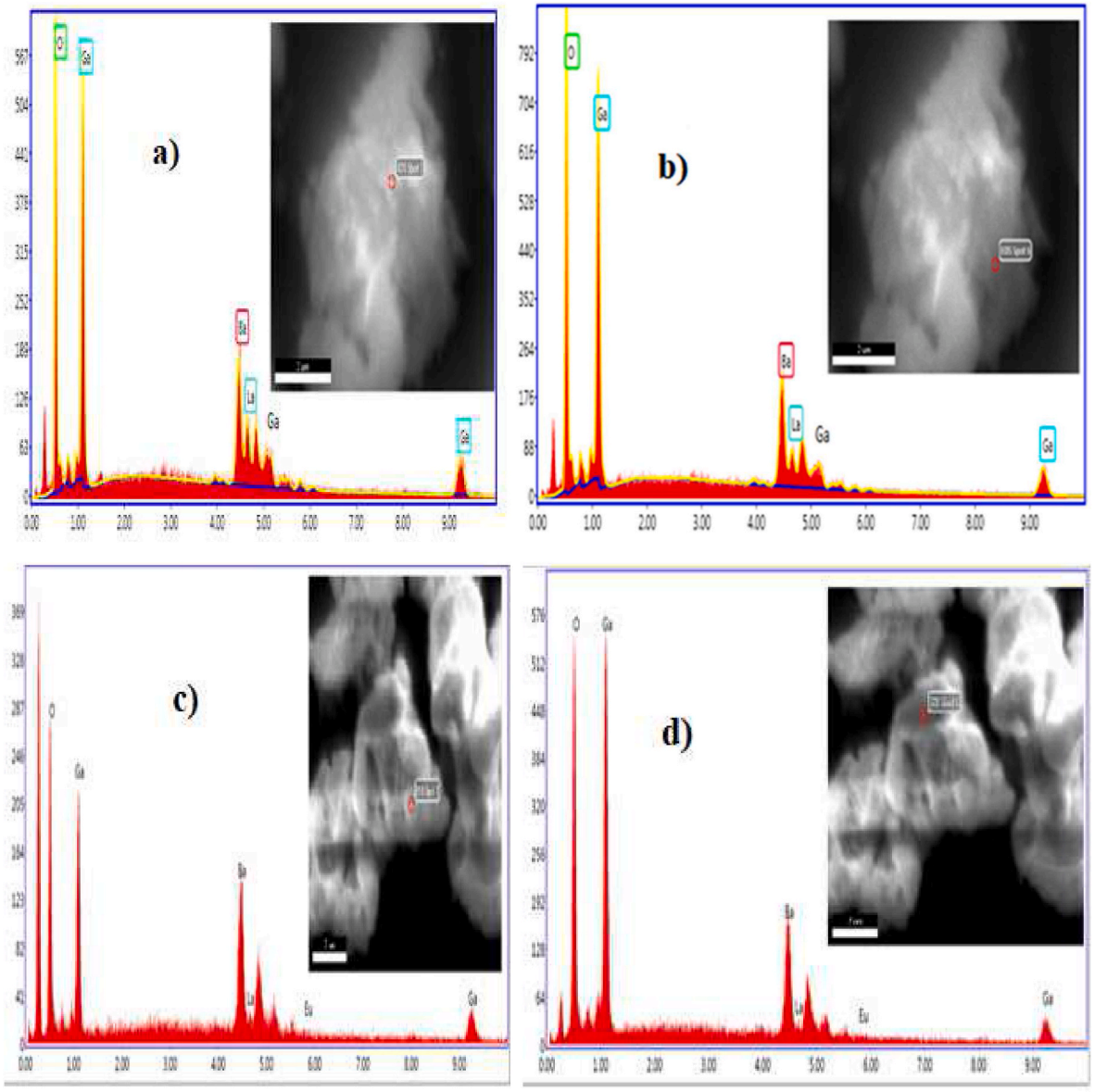

Fig. 3. EDX spectrum (a) at larger grain (b) at smaller grain present in $BaLaGa_3O_7$ phosphor (c) at smaller (d) larger grain of $BaLaGa_3O_7$: 0.05 Eu^{3+} phosphor.

Table: 1
EDX spectral analysis of $BaLaGa_3O_7$ and 0.05 mol % Eu^{3+} ions doped $BaLaGa_3O_7$ phosphors.

Elements	Weight % of elements in (moles)			
	$BaLaGa_3O_7$		$BaLaGa_3O_7$: 0.05 Eu	
	Large grain	Small grain	larger grain	Smaller Grain
O	19.16	20.10	13.65	13.52
Ga	38.53	38.67	33.23	33.52
Ba	31.72	30.61	31.30	31.38
La	10.59	10.62	19.78	19.67
Eu			2.04	1.91

vacancies and it can act as a source for the luminescence in $BaLaGa_3O_7$ phosphor [2,13,49].

Fig. 9 shows the excitation spectra of the $BaLaGa_3O_7$: xEu^{3+} (x = 0.02, 0.05, 0.08, and 0.1) phosphors. The excitation spectra monitored at 616 nm shows a broad band from 250 to 300 nm, which is ascribed to the charge-transfer band (CTB) of Eu^{3+} - O^{2-} together with absorption of host lattice. The region beyond charge transfer band, the sharp excitation peaks are ascribed due to 4f- 4f transitions of Eu^{3+} ion laying in the range 350–500 nm. The peaks recorded at ~310 and ~325 nm are due to $^7F_0 \rightarrow {}^5F_3$ and $^7F_0 \rightarrow {}^5H_3$ transitions. The strongest absorption peak recorded at 374 nm is attributed to the $^7F_0 \rightarrow {}^5L_8$ transitions of Eu^{3+} ions. The excitation at 394 nm corresponds to $^7F_0 \rightarrow {}^5L_6$ transition. The other sharp excitation peaks of Eu^{3+} ions are recorded at 356 ($^7F_0 \rightarrow {}^8G_2$), 412 ($^7F_0 \rightarrow {}^5D_3$), 430 ($^7F_0 \rightarrow {}^5D_3$) and 465 ($^7F_0 \rightarrow {}^5D_2$) nm respectively [50–52].

Fig. 10 shows the emission spectra of $BaLaGa_3O_7$: xEu^{3+}(x = 0.02, 0.05, 0.08, 0.1 mol %) phosphors excited at 374 nm. The discrete emission lines lying between 550 and 750 nm are attributed to the transitions from excited $^5D_0 \rightarrow {}^7F_j$ (j = 0, 1,2,3,4) levels of Eu^{3+} ions. Depending upon the value of j, there are electric dipole and magnetic dipole transitions. The emission lines with even number j favors the electric dipole transitions and is sensitive to the surrounding of Eu^{3+} ions and for the emission lines are with odd number j, the magnetic dipole transitions are generated and it depends on the surroundings [13,15,51]. Three prominent emission peaks are recorded at 537, 613 and 710 nm. The intense peak at 537 nm is attributed to $^7F_1 \rightarrow {}^5D_1$ transitions of Eu^{3+} ion. The weak emission in the region of 580 to 600 nm is

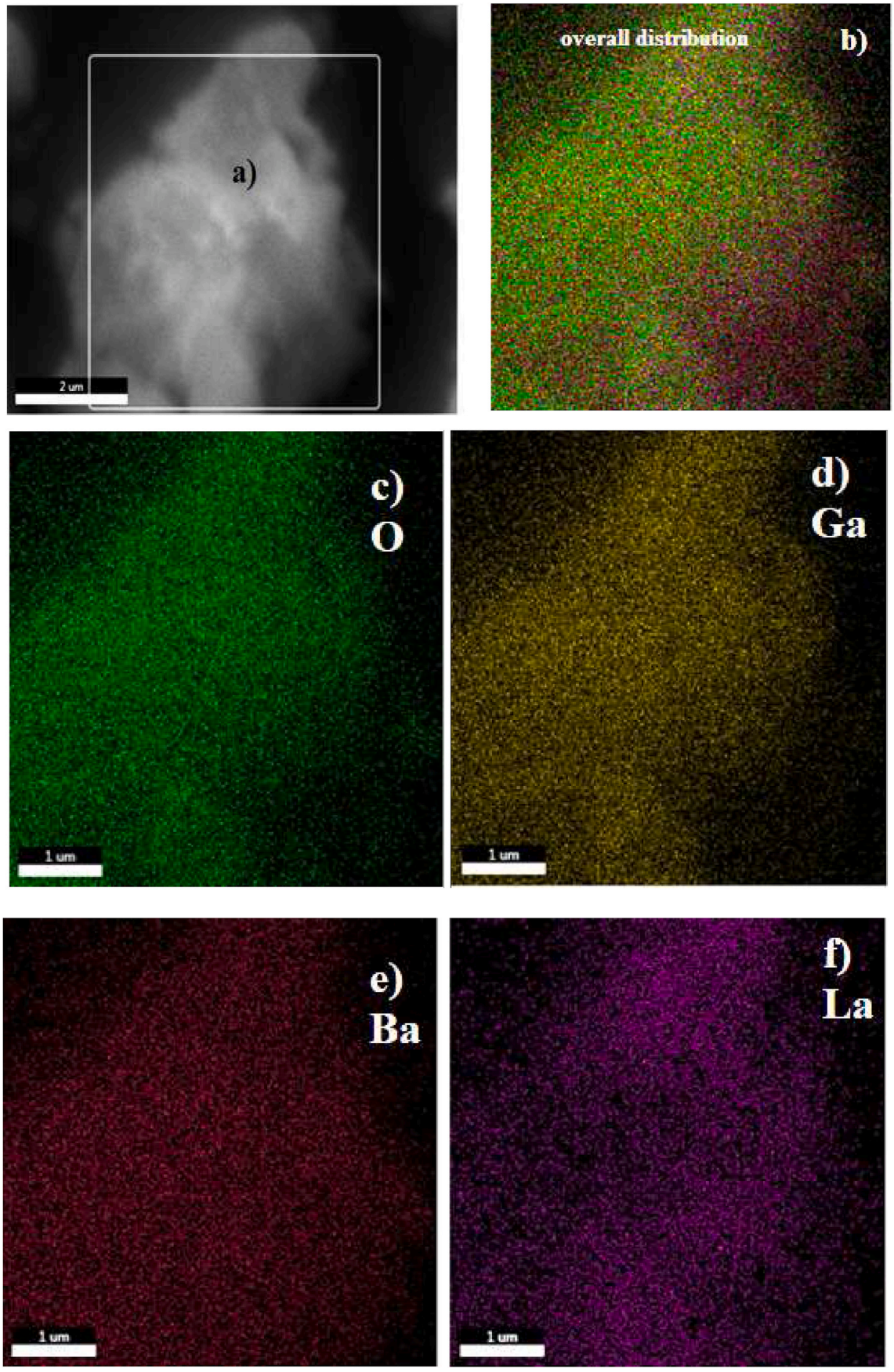

Fig. 4. (a) Elemental mapping area of $BaLaGa_3O_7$ phosphor (b–f) Overall mapping and Elemental mapping of O, Ga, Ba and La present in $BaLaGa_3O_7$ phosphor.

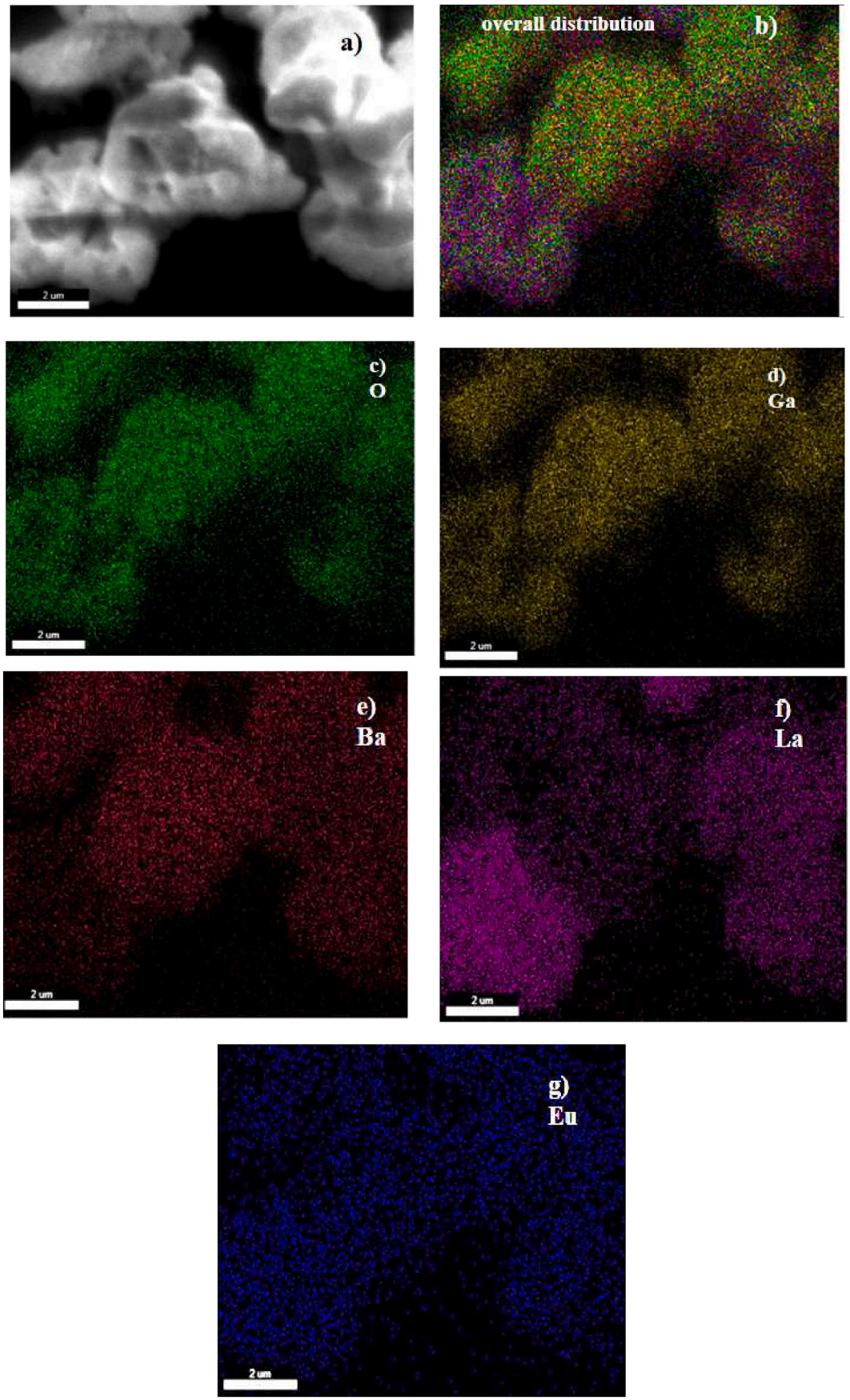

Fig. 5. (a) Elemental mapping area (b) Overall mapping (c–g) Elemental mapping of O, Ga, Ba, La and Eu present in $BaLaGa_3O_7$:0.05Eu^{3+} phosphor.

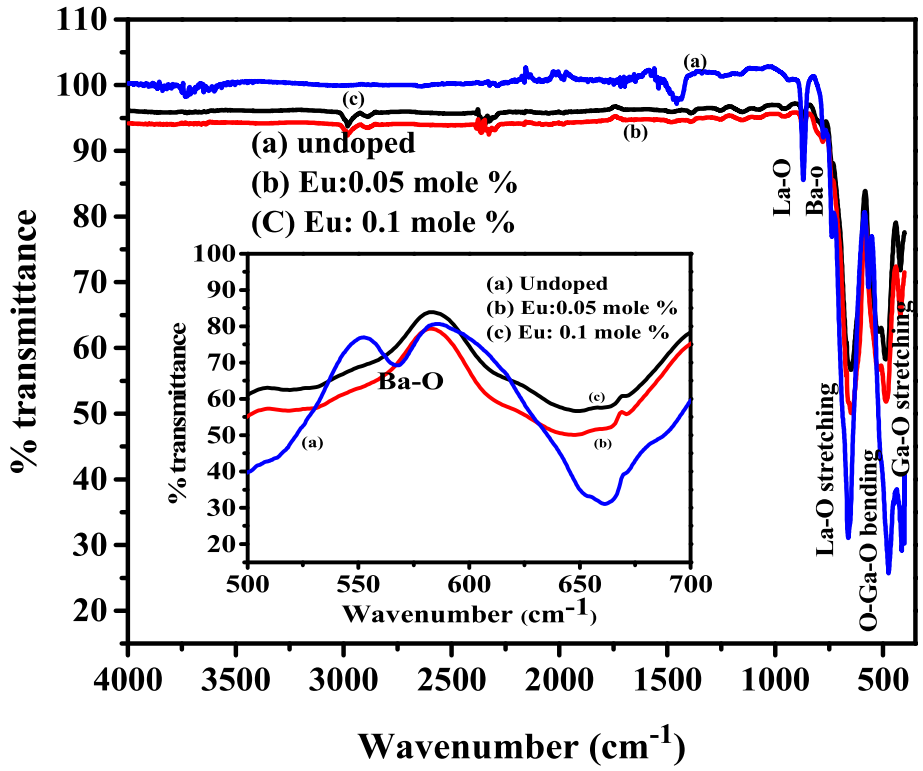

Fig. 6. FTIR Spectra of undoped and Eu^{3+} ions doped $BaLaGa_3O_7$ phosphors.

Table 2
Band assignments of undoped and Eu^{3+} doped $BaLaGa_3O_7$ phosphors.

Wavenumber (cm^{-1})	Band assigned	References
~420	Ga–O bending vibration	33–35
~485	O–Ga - O bending mode	33–35
~525	bands of Ba–O	36
567	Ba–O stretching mode	37–39
~660	La–O stretching vibration	40
~670	Ga–O stretching vibrational mode	34, 35
~740	Stretching and bending of GaO_4 units	33–35
~870	Vibrational bands of La–O bond Ba–O bonds	41, 42

emerged due to the magnetic dipole transition of D and F levels. The peak observed at 587 nm is the typical transition $^5D_0 \rightarrow {}^7F_1$ of Eu^{3+} ions. The intense emission peak assigned at 613 nm is due to the $^5D_0 \rightarrow {}^7F_2$ transition and it provides orange red emission. The weak emission at 663 nm is $^5D_0 \rightarrow {}^7F_3$ transition of europium ion. The peak observed at 686 nm and intense emission peak at 710 nm is due to $^5D_0 \rightarrow {}^7F_4$ transitions [48–50]. The emission color of host phosphor falls in the bluish region and the doping of Eu^{3+} ions leads to the prominent emission peaks in the near red region of the visible spectrum.

Fig. 11 shows the PLE spectra at an excitation of 394 nm. The sharp peak observed at 537 nm is attributed to $^5D_1 \rightarrow {}^7F_1$ transition of Eu^{3+} ion. The most intense red emission peaks at 617 and 650 nm corresponds to the hypersensitive transition between D and F levels due to forced electric dipole $^5D_0 \rightarrow {}^7F_2$ and $^5D_0 \rightarrow {}^7F_3$ transition of Eu^{3+} ions. The emission peaks seen at 570 and 585 nm are attributed to the $^5D_0 \rightarrow {}^7F_0$

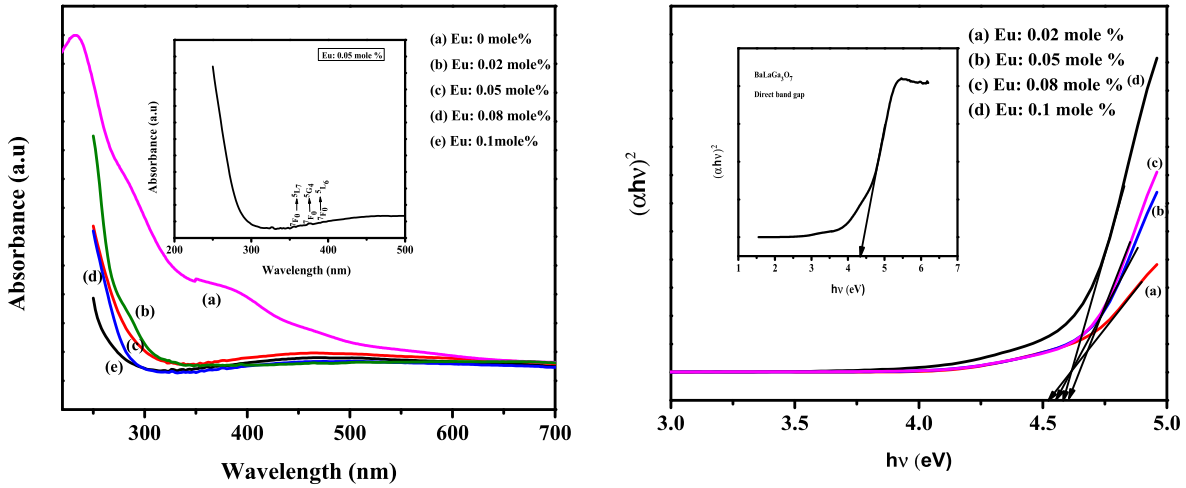

Fig. 7. Absorption spectra of undoped and Eu^{3+} ions doped $BaLaGa_3O_7$ phosphors (a) Direct band gap of undoped and Eu^{3+} ions doped $BaLaGa_3O_7$ phosphors.

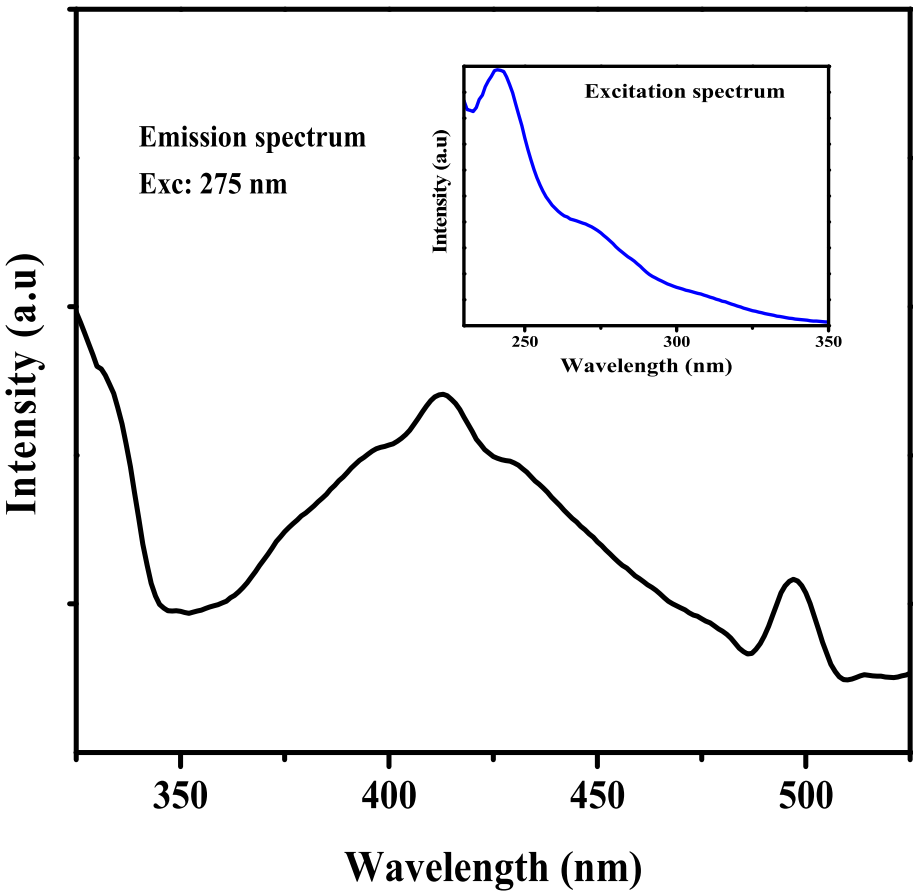

Fig. 8. Emission spectrum of $BaLaGa_3O_7$ phosphor (inset shows the excitation spectrum of $BaLaGa_3O_7$ phosphor).

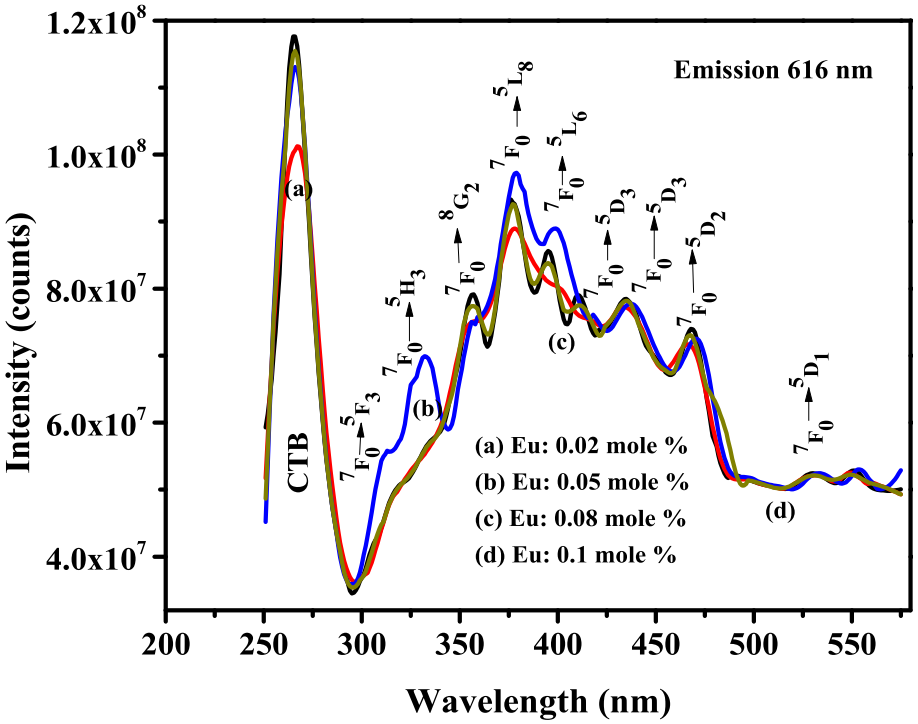

Fig. 9. Excitation spectra of $BaLaGa_3O_7$:xEu^{3+} (x = 0.02, 0.05, 0.08, 0.1 mol %) phosphors.

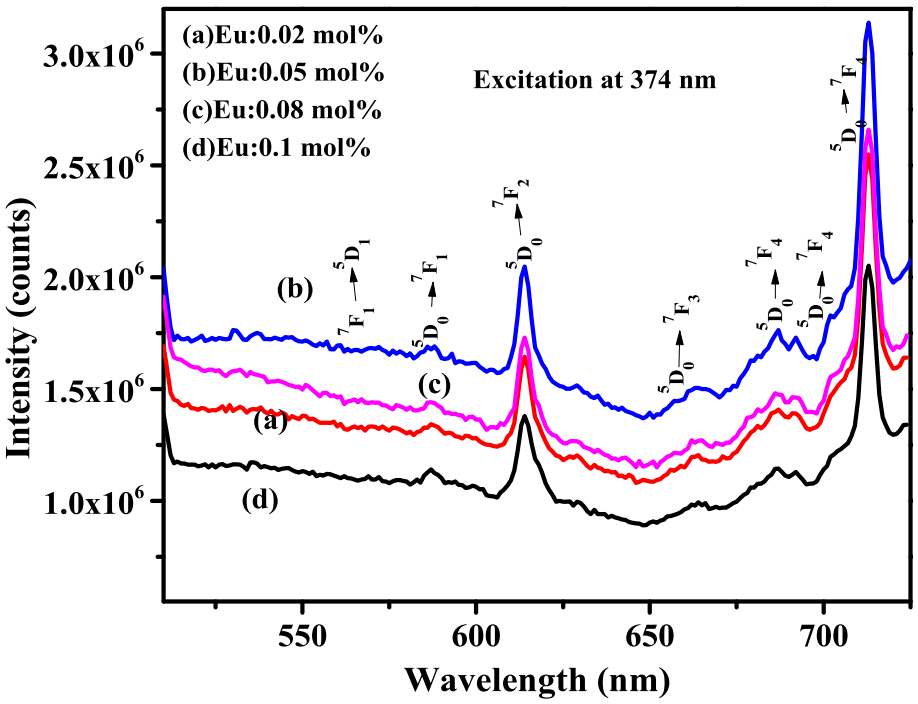

Fig. 10. Emission spectra of $BaLaGa_3O_7:xEu^{3+}$ (x = 0.02, 0.05, 0.08, 0.1 mol %) phosphors excited at 374 nm.

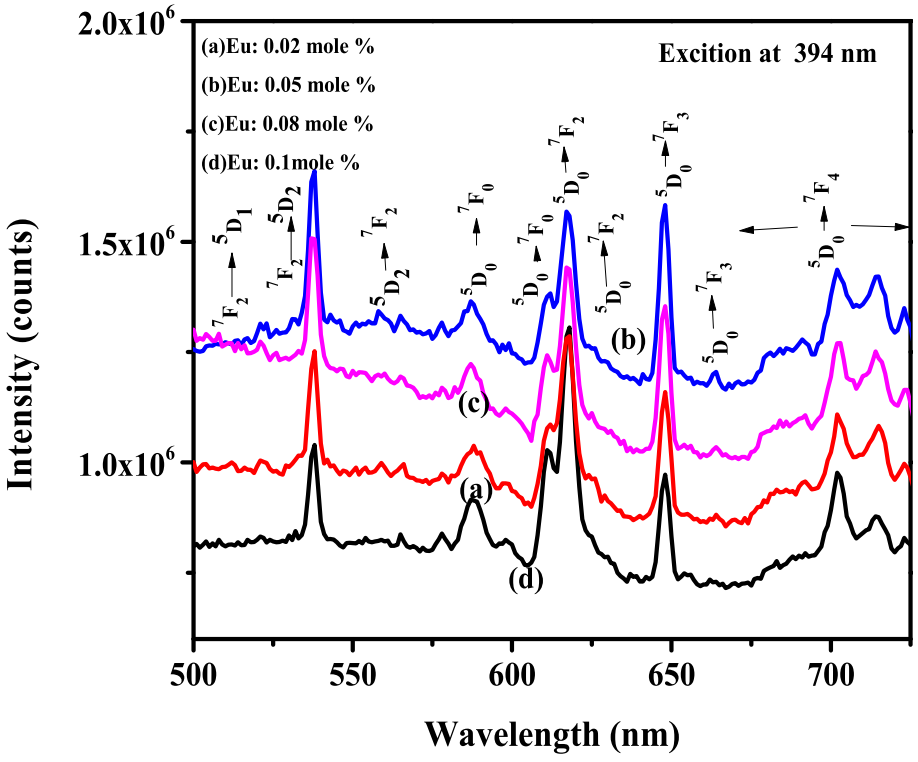

Fig. 11. Emission spectrum of $BaLaGa_3O_7:xEu^{3+}$ (x = 0.02, 0.05, 0.08, 0.1 mol %) phosphors excited at 394 nm.

and $^5D_0 \rightarrow {}^7F_1$ transitions. The emission peaks at 702 and 713 nm are due to $^5D_0 \rightarrow {}^7F_4$ transitions [49–51].

The luminescence spectra show that doping with Eu^{3+} ions cause the enhancement in the relative intensity of $BaLaGa_3O_7$ emission. The PLE spectra show that the intensity of near red emission is stronger when the $BaLaGa_3O_7:Eu^{3+}$ phosphors are excited at 374 nm. The intensity of all the emission peaks excited at 374 nm are higher compared to that excited at 394 nm. The intensity of the excitation and emission peak increases up to 0.05 mol % of Eu^{3+} ions. With further increase in the doping concentration of Eu^{3+} ions quenching of luminescence occurs. Maximum intensity is achieved by 0.05 mol % of Eu^{3+} ion doped $BaLaGa_3O_7$ phosphor.

The performance of a phosphor can be analyzed by studying the chromaticity CIE color coordinates [53]. The chromaticity coordinates

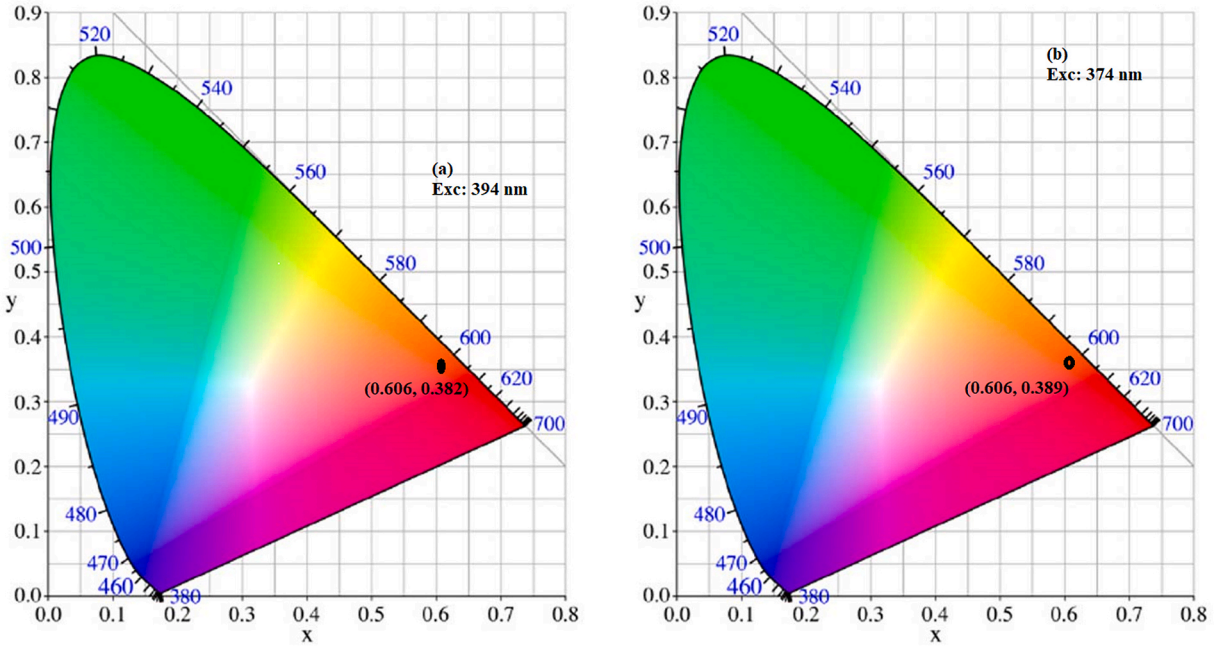

Fig. 12. CIE diagram of $BaLaGa_3O_7$: $0.05Eu^{3+}$ phosphor at an excitation of a) 394 nm b) 374 nm.

of $BaLaGa_3O_7$: $0.05Eu^{3+}$ phosphor excited by 394 and 374 nm are calculated from the corresponding emission spectra and are shown in Fig. 12 (a) and (b).The CIE coordinates are (0.606, 0.382) and (0.602, 0.389) for excitation corresponding to 374 and 394 nm. The chromatic co-ordinates of the luminescence of all phosphors are analyzed and its value reached near red emission [45–48].

From PL spectra and CIE diagram, Eu^{3+} doped barium lanthanum gallate phosphor can be used to control luminescence spectra to get excellent luminophores in visible spectral region of electromagnetic spectrum. $BaLaGa_3O_7$ acts as a promising host matrix and when it is doped with rare earth ions, it can also serve as a component for the phosphor converted WLED's applications [49].

The lifetime measurement is used to study the further luminescence characteristics of phosphors. The term life time indicates the time in which the intensity of a single emission peak becomes 1/e of the original intensity [45–47]. Fig. 13(a–d) show the decay curves of $BaLaGa_3O_7$ phosphors doped with 0.02, 0.05, 0.08 and 0.1 mol % of Eu^{3+} ions excited by a wavelength of 374 nm which corresponds to the emission wavelength of 616 nm. All these phosphors can be well fitted with a single exponential function in decay curve.

$$I(t) = A_0 \exp(-t/\tau) \quad (2)$$

where I is the luminescence intensity, A_0 is a constants, t is the time and τ is the lifetime [45–47]. The life time values corresponding to 0.02, 0.05, 0.08 and 0.1 mol % of Eu^{3+} doped barium lanthanum gallate phosphors are estimated to be 1.28, 1.16, 1.02 and 0.90 ms respectively. As the concentration of Eu^{3+} ions increases, the possibility of quenching centres increases. It enhances non radiative process and it results in the decrease of life time values [24].

3.6. Mechanoluminescence study

The undoped barium lanthanum gallate does not show ML emission even after pre irradiation of gamma rays. But the incorporation of Eu^{3+} dopant on the host matrix exhibits ML emission without the irradiation of any UV or gamma rays. ML emission depends on the nature of the materials, presence of impurities and defects in the lattice of the solids [19]. When the load strikes on the phosphors, it generates the physical and chemical stimulus within the phosphor within a short interval of time. The mechanical stimulus generated the emission of light from the phosphor [17,21,22]. The ML emission of $BaLaGa_3O_7$:xEu^{3+} (x = 0.02, 0.05, 0.08, 0.1 mol %) phosphors are shown in Fig. 14. A single peak is observed in ML intensity versus time curve. This single peak is formed as a result of charge transfer mechanism during the mechanical process. The main reason for the mechanoluminescent activity arises by the release of charge carriers present in the trapped centres at the surface of the phosphor as well as the effect of charge transfer mechanism between the conduction band and holes in the luminescent centre. When the load was dropped on to the surface of the phosphor, some kinds of defects are produced. Such deformation is created by the recombination of dislocation-trapped electrons with the holes in defect centres [19,20,23,24]. ML is excited impulsively, not excited with UV light or gamma rays. So the ML emission may not be related to the trapping and de-trapping of electrons (Chandra, 1998). In this case emission is due to deformation in powder phosphor. It is observed from Fig. 14 that the intensity of glow curve is found to increase with the increase of Eu^{3+} concentration up to 0.05 mol % of Eu^{3+} ions and then decreases for higher concentration of Eu^{3+} ions due to concentration quenching [20,24]. From the measurements of PL and ML, the maximum emission is achieved for 0.05 mol % of Eu^{3+} ions concentration [25]. But position of the ML glow curve remains the same with different concentration of the Eu^{3+} ions.

The experiment is carried out by dropping a 100 g weight from different heights 10, 15 and 20 cm to study the effect of impact velocity on light emission. ML glow curve for $BaLaGa_3O_7$: 0.05% Eu phosphor from different heights shows a good ML peak with better intensity. The intensity of ML peak increases with increase of dropping height and reaches a maximum for a height of 20 cm is shown in Fig. 15. The impact velocity is related to falling height ie, $(2gh)^{1/2}$ [19,24]. When impact velocity increases, piezoelectricity is also increased. When the load is dropped on to the phosphor, the crystallite gets deformed and new defects are produced on the surfaces. These new surfaces cause the generation of piezoelectricity within the phosphor. Due to such piezoelectrification, positive charge is developed in one of the fractured surfaces and other surface becomes negative charge. It allows more number of electrons to get ionized and reach the conduction band and intensity increases [22,23]. The recombination centre will get large number of electrons to be recombined with the holes present in the luminescent centre. This is the major reason for the relation between

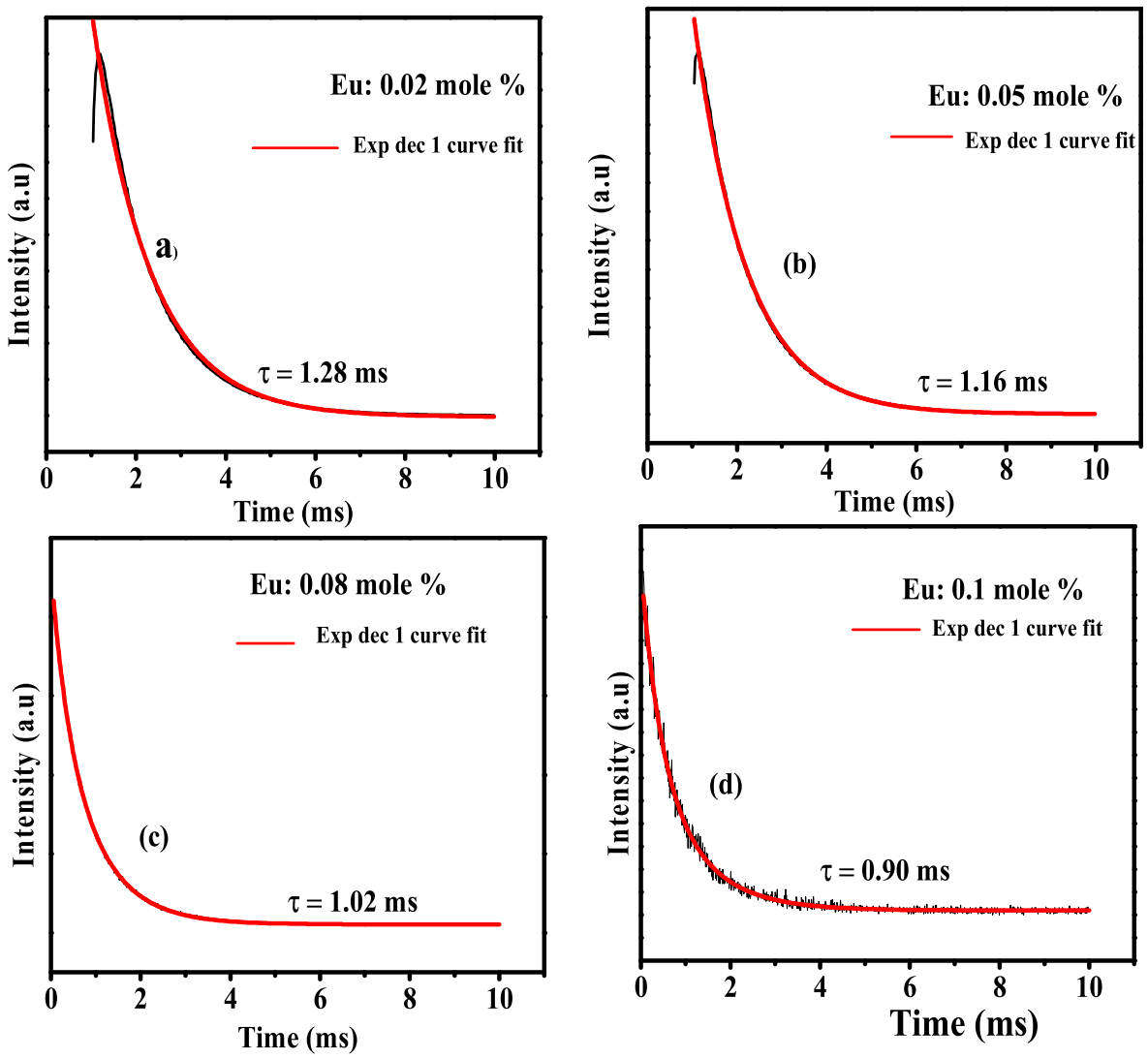

Fig. 13. (a–d): Fitted decay profile of $BaLaGa_3O_7$:xEu^{3+} (x = 0.02, 0.05, 0.08, 0.1 mol %) phosphors.

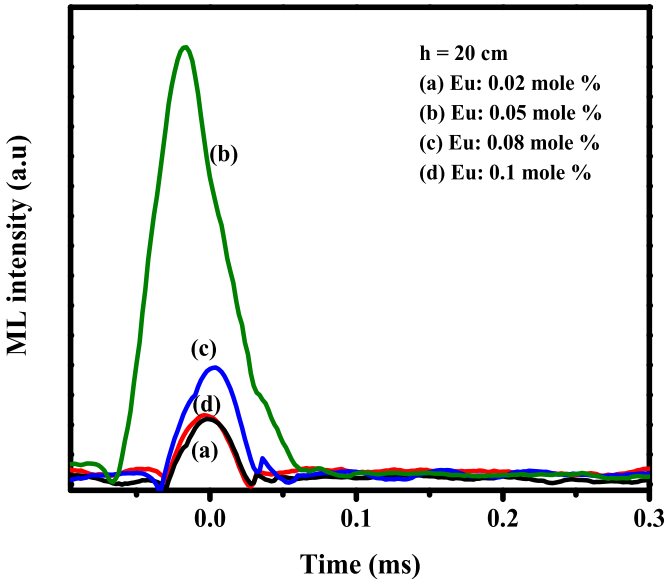

Fig. 14. Variation in ML intensity versus time curve of $BaLaGa_3O_7$: xEu^{3+} (x = 0.02, 0.05, 0.08, 0.1 mol %) phosphors.

increases in peak ML intensity with impact velocity [22–24,56].

3.7. Thermo luminescence (TL)

Thermoluminescence (TL) glow curve of 1 kGy irradiated $BaLaGa_3O_7$ phosphor at a heating rate of 5^0 Cs^{-1} is shown in Fig. 16. A single TL glow curve is obtained at 350 °C. The single peak is formed by the presence of only one type of luminescence centre produced during the gamma irradiation.

3.7.1. Determination of kinetic parameters

The kinetic parameters associated with thermoluminescence depend on the trap levels at different depths in the band gap between the conduction and the valence bands of a material. These levels depend on trap depth, kinetic order of the prepared phosphor and frequency factor [54–56]. The order of kinetics indicates the mechanism of recombination of detrapped charge carriers with their counter parts. The trapping parameters are calculated from TL glow curve using the model developed by Chen. They are Total half intensity width, $\omega = (T_2 - T_1)$, High temperature half width, $\delta = (T_2 - T_m)$ and Low temperature half width, $\tau = (T_m - T_1)$, where T_m is the maximum peak temperature [28].

The shape factor usually helps to determine the order of kinetics. It can be calculated using the equation $\mu_g = \delta/\omega$. ie, $(T_2 - T_m)/(T_2 - T_1)$ [28, 55,56].

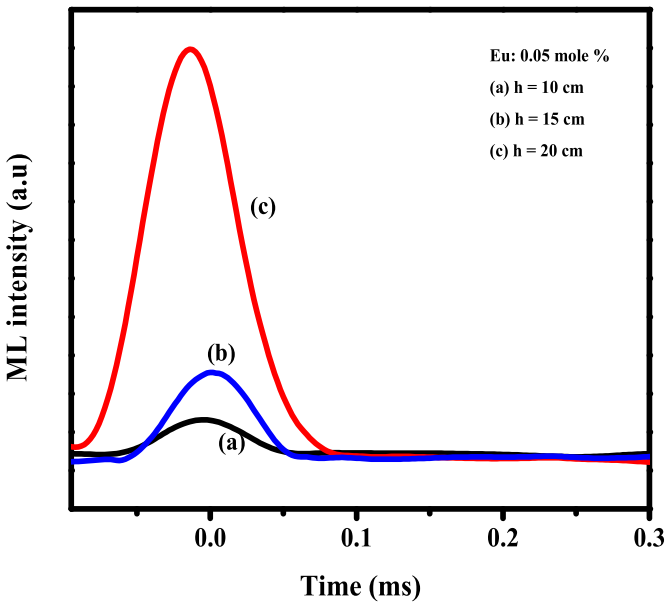

Fig. 15. Variation in ML intensity versus time curve for different dropping heights (h = 10, 15, 20 cm) in $BaLaGa_3O_7$:0.05Eu^{3+} phosphor.

$\mu_g = 0.42$ *for first order kinetics*
$\mu_g = 0.52$ *for second order kinetics*

The calculated shape factor of the prepared $BaLaGa_3O_7$ phosphor from Chen's method is found to be 0.444. It reveals that prepared phosphor is first order of kinetics [22,24]. The value of shape parameters are listed in Table 3.

3.7.2. Trap depth E

Trap depth calculation is used to determine the amount of an element present in the phosphor. Some kinds of impurities, presence of vacant lattice sites and lattice structural defects, provide unoccupied energy levels called traps. If the traps are deep enough, the charge carriers will be retained for a long period of time even after the irradiation is removed.

Activation energy E corresponding to first order of kinetics can be calculated using the equation [22,24,55,56].

$$E = 2kT_m\left[1.76\left(T_m/\omega\right) - 1\right] \tag{3}$$

From equation (3) the activation energy is calculated to be 1.107 eV. The trap depth E in terms of ω, δ, τ can also be calculated using the equation

$$E_\Upsilon = c_\Upsilon\left(\frac{kT_m^2}{\Upsilon}\right) - b_\Upsilon\left(2kT_m\right) \tag{4}$$

where Υ is ω, δ, τ. The constants c_ω, c_δ, c_τ, b_ω, b_δ, b_τ for first order kinetics are calculated using the equations [28,57].

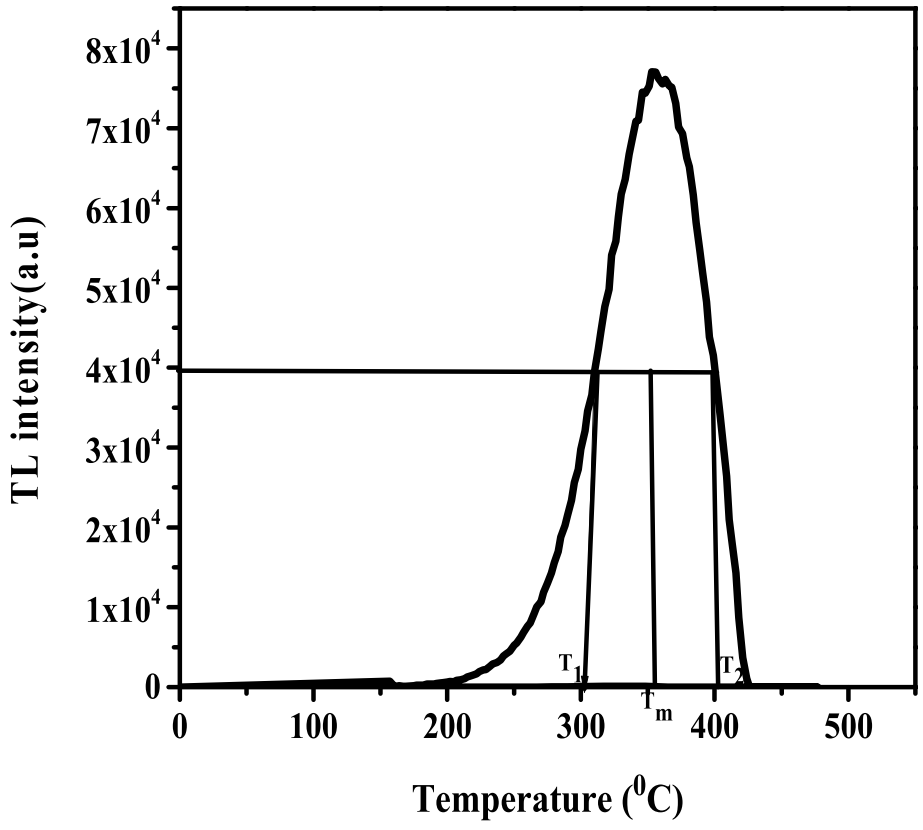

Fig. 16. TL Glow curve of $BaLaGa_3O_7$ phosphor.

Table 3
Kinetic parameters of $BaLaGa_3O_7$ phosphor.

T_I (°C)	T_2 (°C)	T_m (°C)	ω (T_2-T_1)	δ (T_2-T_m)	τ (T_m - T_1)	μ (δ/ω)	E_ω (eV)	E_τ (eV)	E_δ (eV)
302	401	357	99	44	**55**	0.44	1.0496	1.156	0.872

$$B_\tau = 1.58 + 4.2(\mu - 0.42) \quad (5)$$

$$c_\tau = 1.510 + 3(\mu - 0.42) \quad (6)$$

$$c_\delta = 0.976 + 7.3\ (\mu - 0.42) \quad (7)$$

$$c_\omega = 2.52 + 10.2(\mu - 0.42) \quad (8)$$

From (5) (6) (7) and (8), the values of the constants are calculated to be c_ω = 2.724, c_τ = 1.57, c_δ = 1.122, b_τ = 1.664, b_ω = 1, b_δ = 0 respectively. Using these values, trap depth energies from equation (4) are found to be 1.049, 1.15, 0.87eV corresponding to E_ω, E_τ and E_δ respectively. Trap depth parameters are tabulated in Table 3.

4. Conclusions

$BaLaGa_3O_7$:xEu^{3+} (x = 0, 0.02, 0.05, 0.08, 0.1 mol %) ceramic phosphors have been synthesized using solid state reaction method. XRD patterns reveal that the prepared undoped and doped phosphors are single phase and no characteristic peaks of Eu_2O_3 are identified. FESEM analysis shows that the synthesized compounds are made up of two different sized particles - small particles with size around 1–3 μm and large particles with an average size of about 2–5 μm respectively. The EDX spectra confirmed that the two different shaped particles are of same composition. The elemental mapping provides the presence all constituent elements and homogeneous distribution of elements on the surface of the phosphors. FTIR analysis confirms the vibrational modes present in the phosphors. The direct band gap energies of Eu^{3+} doped barium lanthanum gallate phosphor lie in the range 4.5–4.6 eV. The increment in the band gap energy with dopant concentration is due to Burstein – Moss effect. The undoped phosphor exhibits strong excitation peak at 275 nm. The emission spectrum shows strong emission peaks at 413 nm and 495 nm corresponding to the bluish region of the visible spectrum. The emission is attributed to the presence of Ga^{3+} ions in the host matrix. The excitation spectra of the $BaLaGa_3O_7$: xEu^{3+} phosphors monitored with emission wavelength of 617 nm exhibit sharp excitation peaks in the range 350–500 nm due to 4f- 4f transitions of Eu^{3+} ions. The prominent excitation peaks are recorded at 374 and 394 nm attributed to the $^7F_0 \rightarrow {}^5L_8$ and $^7F_0 \rightarrow {}^5L_6$ transitions of Eu^{3+} ions and other sharp excitation peaks of Eu^{3+} ions assigned at 362, 382, 412 and 465 nm. The emission spectra corresponding to excitation of 374 nm gives three sharp emission peaks at 537, 613 and 710 nm ascribed to Eu^{3+} transitions. The emission spectra corresponding to 394 nm exhibits intense red emission peaks at 617 and 650 nm and are attributed to electric dipole transition of Eu^{3+} ions. The other emission peaks are recorded at 570, 585, 702 and 713 nm. The emission spectra corresponding to both the excitations show maximum emission for 0.05 mol % of Eu^{3+} dopant concentration. Beyond that concentration, quenching of luminescence occurs. The emission characteristics of this phosphor reveal that it can be probably used as a candidate for the phosphor converted WLED's applications. The lifetime values of Eu^{3+} ions at different concentrations (x = 0.02, 0.05, 0.08 and 0.1) has been determined to be about 1.28, 1.16, 1.02 and 0.90 ms respectively. The Eu^{3+} ions doped $BaLaGa_3O_7$ exhibit excellent mechanoluminescence emission. The ML emission enhances with impact velocity and with Eu^{3+} ion concentration. For PL and ML studies the maximum intensity is recorded for 0.05 mol % of Eu^{3+} ions. Beyond that concentration intensity decreases due to concentration quenching. From these luminescence studies 0.05 mol% of Eu^{3+} doped $BaLaGa_3O_7$ phosphor can be used for phosphor's converted WLED's, solid state light emitting diodes, sensors and stress indicators applications. The thermoluminescence spectrum of 1 kGy irradiated undoped barium lanthanum gallate shows good thermoluminescence emission without any dopants. A single low temperature peak is observed from TL curve similar to that recorded in ML emission. This single peak is due to the presence of one type of luminescence center existing in the phosphor. The shape factor calculated using Chen's method is found to be 0.44 and hence it is first order of kinetics with activation energy 1.107 eV.

Authorship statement

Conception and design of study: N. Gopakumar, P. S. Anjana, Acquisition of data: B. Vasanthi, Analysis and/or interpretation of data: B. Vasanthi, N. Gopakumar, P. S. Anjana, Drafting the manuscript: B. Vasanthi, Revising the manuscript critically for important intellectual content: N. Gopakumar, P. S. Anjana, Approval of the version of the manuscript to be published: B. Vasanthi, N. Gopakumar, P. S. Anjana.

Declaration of competing interest

The authors declare that they have no known competing financial interests or personal relationships that could have appeared to influence the work reported in this paper.

Acknowledgments

The authors are thankful to the Department of Physics, University of Kerala for the X-ray diffraction studies. The authors are grateful to Dr. K. G. Gopchandran, Department of Optoelectronics, University of Kerala for FTIR, FESEM, UV–Visible studies and Photoluminescence analysis. The authors are grateful to CLIF, University of Kerala for EDX elemental mapping and decay studies. The authors are thankful to Dr. Panigrahi, IGCAR, Kalpakkam, for TL characterization. The authors are grateful to Directorate of Collegiate Education, Government of Kerala for the ASPIRE fellowship. This research did not receive any specific grant from funding agencies in the public, commercial, or not-for- profit sectors.

References

[1] M. Berkowski, M.T. Borowiec, K. Pataj, W. Piekarczyk, W. Wardzynski, Absorption and birefrigence of $BaLaGa_3O_7$ single crystals, Physica 123 B+C (1984) 215–219, https://doi.org/10.1016/0378-4363(84)90126-8.

[2] Junling Meng, Xiaojuan Liu, Congting Sun, Chuangang Yao, Lifang Zhang, Fen Yao, Dongfeng Xue, Jian Meng, Hongjie Zhang, Luminescence mechanistic study of BaLaGa3O7:Nd using density functional theory calculations, Inorg. Chem. 55 (2016) 2855–2863, https://doi.org/10.1021/acs.inorgchem.5b02714.

[3] Beibei Liu, Weiwei Guo, Fanglin Chen, Changron Xia, Ga site doping and concentration variation effects on the conductivities of melilite type lanthanum strontium gallate electrolytes, Int. J. Hyd. energy 37 (2012) 961–966, https://doi.org/10.1016/j.ijhydene.2011.03.093.

[4] Michael Rozumek, Peter Majewski, Linda Sauter, Aldinger Fritz, $La_{1+x}Sr_{1-x}Ga_3O_{7-\delta}$ melilite type ceramics: preparation, composition, and structure, J. Am. Ceram. Soc. 87 (4) (2004) 662–669, https://doi.org/10.1111/j.1551-2916.2004.00662.x.

[5] W. Ryba - Romanowski, B. Jesowska, Trzebia -Towska, Optical properties and lasing of BaLaGa3O7 single crystals doped with neodymium, J.Phys. Chem. Solids 49 (2) (1988) 199–203, https://doi.org/10.1016/0022-3697(88)90051-0.

[6] W. Ryba - Romanowski, S. Golab, G. Dominiak- Dzik, Effect of substitution of barium by strontium on optical properties of neodymium doped $XLaGa_3O_7$ (X= Ba, Sr), Mater.Sci. Engg B15 (1992) 217–221, https://doi.org/10.1016/0921-5107(92)90061-D.

[7] I. Pracka, W. Giersz, M. Świrkowicz, A. Pajaczkowsk, S. Kaczmarek, Z. Mierczyk, K. Kopczyński, The Czochralski growth of SrLaGa3O7 single crystals and their optical and lasing properties, Mater. Sci. Eng. B 26 (Issues 2–3) (1994) 201–206, https://doi.org/10.1016/0921-5107(94)90172-4.

[8] W. Piekarczyk, M. Berkowski, G. Jasiolek, The Czochralski growth of BaLaGa3O7 single crystal, J. Cryst. Growth 71 (1985) 395–398, https://doi.org/10.1016/0022-0248(85)90097-1.

[9] M. Karbowiak, P. Gnutek, C. Rudowicz, W. Ryba - Romanowski, Crystal - field analysis for RE^{3+} ions in laser materials: 11. Absorption spectra and energy levels calculations for Nd^{3+} ions doped into $SrLaGa_3O_7$ and $BaLaGa_3O_7$ crystals and Tm^{3+} ions in$SrGdGa_3O_7$, Chem. Phys. 387 (2011) 69–78, https://doi.org/10.1016/J.CHEMPHYS.2011.06.036.

[10] S.I. Stepanov, V.I. Nikolaev, V.E. Bougrov, A.E. Romanov, Gallium oxide: properties and applications - a review, Rev. Adv. Mater. Sci. 44 (2016) 63–86.

[11] Kh M. Al-khamis, Refaat M. Mahfouz, Abdulrahman A. Al-warthan , Synthesis and characterization of gallium oxide nanoparticles, Arabian J. Chem. 2 (2009) 73–77, https://doi.org/10.1016/j.arabjc.2009.10.001.

[12] Mohd Saleem, Riya Neema, M. Mittal, P.K. Sharma, Mechanoluminescence of rare-earth doped aluminate phosphors - a review, Int. J. Sci. Res. Phys. Appl Sci. 3 (3) (2015) 4–10. ISSN 2348-3423.

[13] Shuxin Liu, Shuwei Ma, Shuxian Wang, Zhengmao Ye, Exploring crystal-field splittings of Eu^{3+} ions in γ- and β-$SrGa_2O_4$, J. Lumin. 210 (2019) 155–163, https://doi.org/10.1016/j.jlumin.2019.02.027.

[14] R. Bazzi, M. A Flores, C. Louis, K. Lebbou, W. Zhang, S. Roux, Synthesis and properties of europium based phosphors on the nanometer scale: Eu_2O_3, Gd_2O_3: Eu and Y_2O_3: Eu, J. Colloid Interface Sci. 273 (2004) 191–197, https://doi.org/10.1016/j.jcis.2003.10.031.

[15] Jens Adam, Wilhelm Metzger, Marcus Koch, Rogin Peter, Toon Coenen, Jennifer S. Atchison, König Peter, Light emission intensities of luminescent Y_2O_3:Eu and Gd_2O_3:Eu particles of various sizes, J. Nanomater. 7 (2017) 26–34, https://doi.org/10.3390/nano7020026.

[16] Ayush Kharea, B. Nag Bhargavi, Namrata Chauhan, Nameeta Brahme, Thermo and mechanoluminescence studies of BZT phosphor, Optik 125 (2014) 4655–4658, https://doi.org/10.1016/j.ijleo.2014.04.091.

[17] B.P. Chandra, V.K. Chandra, Piyush Jh, Models for intrinsic and extrinsic fracto mechanoluminescence of solids, J. Lumin. (2013) 139–153, https://doi.org/10.1016/j.ijleo.2014.04.091.

[18] Shilpa A. Pardhi, Govind B. Nair, Ravi Sharma, S. J Dhoble, Investigation of thermoluminescence and electron-vibrational interaction parameters in $SrAl_2O_4$: Eu^{2+}, Dy^{3+}phosphors, J. Lumin. 187 (2017) 492–498, https://doi.org/10.1016/j.jlumin.2017.03.028.

[19] S. J Sajan, N. Gopakumar, P. S Anjana, K. Madhukumar, Synthesis, characterization and mechanoluminescence of europium doped Zn(x)Ba(1-x)Al_2O_4 (x = 0, 0.4, 0.5, 0.6, 0.8, 1.0) phosphor, J. Lumin. 174 (2016) 11–16, https://doi.org/10.1016/j.jlumin.2016.01.024.

[20] S. J Sajan, N. Gopakumar, P. S Anjana, R. S Kher, Revupriya, Synthesis, characterization and mechanoluminescence properties of europium doped (1-x) MgO.xBaO- Al2O3:0.1 Eu(x = 0,0.2,0.4,0.5,0.6,0.8,1.0) phosphor, Optik 156 (2018) 921–928, https://doi.org/10.1016/j.ijleo.2017.11.193.

[21] P. Jha, B.P. Chandra, Impulsive excitation of mechanoluminescence in $SrAl_2O_4$:Eu, Dy phosphors prepared by solid state reaction technique in reduction atmosphere, J. Lumin. 143 (2013) 280–287, https://doi.org/10.1016/j.jlumin.2013.05.011.

[22] Ishwar Prasad Sahu, D. P Bisen, Raunak Kumar Tamrakar, K.V.R. Murthy, M. Mohapatra, Luminescence studies on the europium doped strontium metasilicate phosphor prepared by soild state reaction method, J. Sci. Adv. Mater Devices 2 (2017) 59–68, https://doi.org/10.1016/j.jlumin.2013.05.011.

[23] Ravi Shrivastava, Jagjeet Kaur, Characterization and mechanoluminescence studies of $Sr_2MgSi_2O_7$:Eu^{2+},Dy^{3+}, J. Rad. Res. Appl. Sci. 8 (2015) 201–207, https://doi.org/10.1016/j.jrras.2015.01.005.

[24] Ishwar Prasad Sahu, D. P Bisen, Raunak Kumar Tamrakar, K.V.R. Murthy, M. Mohapatra, Studies on the Luminescence Properties of $CaZrO_3$:Eu^{3+} phosphors prepared by the solid state reaction method, J. Sci. Adv. Mater. Devices 2 (1) (2017) 69–78, https://doi.org/10.1016/j.jsamd.2017.01.002.

[25] S. Sailaja, S.J. Dhoble, Nameeta Brahme, B. Sudhakar Reddy, Synthesis, Photoluminescence and mechanoluminescence properties of Eu^{3+} ions activated $Ca_2Gd_2W_3O_{14}$ phosphors, J. Mater. Sci. 46 (2011) 7793–7798, https://doi.org/10.1007/s10853-011-5759-2.

[26] Juan Azorín Nieto, Thermoluminescence of metallic oxides. Development and applications in Mexico: an overview, Appl. Radiat. Isot. 138 (2018) 35–39, https://doi.org/10.1016/j.apradiso.2017.07.044.

[27] R.K. Rai, A.K. Upadhyay, R.S. Kher, S.J. Dhoble, Mechanoluminescence, thermoluminescence and photoluminescence studies on Al_2O_3:Tb phosphors, J. Lumin. 132 (2012) 210–214, https://doi.org/10.1016/j.jlumin.2011.08.003.

[28] Nameeta Brahme Tiwari, Ravi Sharma, D.P. Bisen, Sanjay K. Sao, Fracto-mechanoluminescence and thermoluminescence properties of orange-red emitting Eu^{3+} doped $Ca_2Al_2SiO_7$ phosphors, J. Lumin. 183 (2017) 89–96, https://doi.org/10.1016/j.jlumin.2016.11.012.

[29] Vikas Dubeya, Jagjeet Kaura, Sadhana Agrawal, N.S. Suryanarayana, K.V. R. Murthy, Synthesis and characterization of Eu^{3+} doped SrY_2O_4 phosphor, Optik 124 (2013) 5585–5587, https://doi.org/10.1016/j.ijleo.2013.03.153.

[30] Peter Majewski, Michael Rozumek, A. Cuneyt, Tas, Fritz Aldinger, processing of (La,Sr)(Ga,Mg)O_3 solid electrolyte, J. Electr. ceram. 8 (1) (2002) 65–73, https://doi.org/10.1023/A:1015507520661.

[31] Shufang Gao, Shan Xu, Yeqing Wang, Chaoyang Tu, Spectral characteristics and white emission of Dy3+/Tm3+-BaLaGa3O7 phosphors, J. Lumin. 178 (2016) 282–287, https://doi.org/10.1016/j.jlumin.2016.05.040.

[32] R. Ashiri, Detailed FT- IR spectroscopy characterization and thermal analysis of synthesis of barium titanate nanoscaleparticles through a newly developed process, Vib. Spectrosc. 66 (2013) 24–29, https://doi.org/10.1016/j.vibspec.2013.02.001.

[33] Musa Mutlu Can, G. Hassnain Jaffari, Seda Aksoy, S. Ismat Shah, Tezer Firat, Synthesis and characterization of $ZnGa_2O_4$ particles prepared by solid state reaction, J.alloys. Comp. 549 (2013) 303–307, https://doi.org/10.1016/j.jallcom.2012.08.137.

[34] Amba Mondal, Sourav Das, J. Manam, Hydrothermal synthesis, structural and luminescent properties of a Cr^{3+}doped $MgGa_2O_4$ near-infrared long lasting nanophospor, RSC Adv. 6 (2016) 82484, https://doi.org/10.1039/C6RA15119A.

[35] T.A. Safeera, N. Johns, K. Mini Krishna, P.V. Sreenivasan, R. Reshmi, E.I. Anila, Zinc gallate and its starting materials in solid state reaction route- A comparative study, Mater. Chem. Phys. (2016) 1–5, https://doi.org/10.1016/j.matchemphys.2016.06.029.

[36] Atul Shah, B. Patel, FTIR and XRD study of barium tartrate (BaC_4H_4O6) crystals grown by gel method, AIP Conference proceedings 1249 (2010) 192, https://doi.org/10.1063/1.3466554.

[37] E. Sundharam, A. Kingson Solomon Jeevaraj, C. Chinnusamy, Effect of ultrasonication on the synthesis of barium oxide nanoparticles, J. Bio. nano.sci. 11 (2017) 310–314, https://doi.org/10.1166/jbns.2017.1449.

[38] Saeed Aly, Y.H. Elbashar, S.U. El Khameesy, A novel barium borate glasses for optical applications, Siliconindia 10 (2018) 569–574, https://doi.org/10.1007/s12633-016-9492-y.

[39] S. Abramowitz, N. Acquista, The infrared spectrum of matrix isolated BaO_2, J. Res. the National Bureau of Standards, Phys. Chem. 75A (No.1) (1971).

[40] M. F Faznny, M.K. Halimah, M.N. Azlan, Effect of Lanthanum oxide on optical properties of Zinc boro tellurite glass system, J. Optoelect.Biomed.Mater. 8 (2) (2016) 49–59.

[41] Amanullakhan A. Pathan, Kavita R. Desai, C.P. Bhasin, Synthesis of La_2O_3 Nanoparticles using Glutaric acid and Propylene glycol for future CMOS applications, Int. J. Chem. 3 (2) (2017) 21–25, https://doi.org/10.18576/ijnc/030201.

[42] Eva Roedel, Atsushi Urakawa, Sven Kuretiwand Alfons Baiker, On the local sensitivity of different IR techniques: Ba species relevant in NOx storage-reduction, Phys. Chem. Chem. Phys. 10 (2008) 6190–6198, https://doi.org/10.1039/B808529C.

[43] Timur Sh Atabaev, Yoon - Hwae Hwang, Hyung - Kook Kim Atabaev, Color-tunable properties of Eu^{3+} and Dy^{3+} codoped Y_2O_3 phosphor particles, Nanoscale Res. Lett. 7 (2012) 556, https://doi.org/10.1186/1556-276X-7-556.

[44] Patrycja Makuła, Michał Pacia, Wojciech Macyk, How to correctly determine the band gap energy of modified semiconductor photocatalysts based on UV−Vis Spectra, J. Phys. Chem. Lett. 9 (23) (2018) 6814–6817, https://doi.org/10.1021/acs.jpclett.8b02892.

[45] R. Raji, R.G. Abhilash Kumar, K.G. Gopchandran, Influence of local structure on luminescence dynamics of red emitting ZnO: Eu^{3+} nanostructures and its Judd-Ofelt analysis, J. Lumin. 205 (2019) 179–189, https://doi.org/10.1016/j.jlumin.2018.09.002.

[46] Padmini Pandey, Rajnish Kurchania, Fozia Z. Haque, Optical studies of europium-doped ZnO nanoparticles prepared by Sol–Gel technique, J. Adv. Phys. 3 (2) (2014) 1–7, https://doi.org/10.1166/jap.2014.1120.

[47] T. Samuel, Ch Satya Kamal, K. Sujatha, V. Veeraiah, Y. Ramakrishana, K. Ramachandra Rao, Photoluminescence enhancement and energy transfer mechanism of Bismuth added $LaGaO_3$: Eu nanophosphor for display applications, Optik 127 (2016) 10575–10587, https://doi.org/10.1016/j.ijleo.2016.08.063.

[48] Serdar Yildirim, Selim Demirci, Kadriye Ertekin, Erdal Celik, Zumre Arican Alicikus, Production, characterization, and luminescent properties of Eu^{3+}doped yttrium niobate–tantalate films, J. Adv Ceram. 6 (1) (2017) 33–42, https://doi.org/10.1007/s40145-016-0215-z.

[49] Hai Liu, Lixin Yu, Fuhai Li, Photoluminescence properties of Eu^{3+} and Dy^{3+} doped $MgGa_2O_4$ phosphors, J. Phys. Chem. Solid. 74 (2013) 196–199, https://doi.org/10.1016/j.jpcs.2012.09.006.

[50] Baoxing Wang, Qiang Ren, Hai Ou, Xiulan Wu, Luminescence properties and energy transfer in Tb^{3+} and Eu^{3+} co-doped $Ba_2P_2O_7$ phosphors, RSC Adv. 7 (2017) 15222, https://doi.org/10.1039/C6RA28122B.

[51] Koen Binnemans, Interpretation of europium (III) spectra, Coord. Chem. Rev. 295 (2015) 1–45, https://doi.org/10.1016/j.ccr.2015.02.015.

[52] M.J. Oh, H. J Kim, Synthesis and luminescent properties of $Gd_3Ga_2Al_3O_{12}$ phosphors doped with Eu^{3+} or Ce^{3+}, J. Kor. Phys. Soc. 69 (2016) 1110–1114, https://doi.org/10.3938/jkps.69.1110.

[53] Pushpa Kumari, Y. Dwivedi, Vibrational and spectroscopic analysis of white light emitting Bi_2SiO_5 nanophosphor, Spectrochim. Acta, Part A: Mole. Biomol. Spectrosc. 180 (2017) 79–84, https://doi.org/10.1016/j.saa.2017.03.005.

[54] Neha Tiwari, Raunak Kumar Tsmrakar, Mechanoluminescence, photoluminescence and thermoluminescence studies of $SrZrO_3$: Ce phosphor, J. Rad. res. Appl. Sci. 8 (2015) 68–76, https://doi.org/10.1016/j.jrras.2014.11.002.

[55] Jagjeet Kaur, Yogita Parganiha, Vikas Dubey, Luminescence studies of Eu^{3+}Doped calcium bromofluoride phosphor, Physics Research International (2013), https://doi.org/10.1155/2013/494807. Article ID 494807, 2013, 5pages.

[56] R. Chen, V. Pagonis, J.L. Lawless, Evaluated thermoluminescence trapping parameters , what do they really mean? Radiat. Meas. 91 (2016) 21–27.

[57] Raunak Kumar Tamrakar, Durga Prasad Bisen, Kanchan Upadhyay, Samit Tiwari, Synthesis and thermoluminescence behavior of ZrO_2:Eu^{3+} with variable concentration of Eu^{3+}doped phosphor, J. Rad. Res and Appl.Sci. 7 (2014) 486–490, https://doi.org/10.1016/j.jrras.2014.08.006.